The damping effect of magnetorheological elastomers on dynamic absorber for powertrain vibration reduction

Nga Hoang[*,***], Nong Zhang[*] and Haiping Du[**]

*School of Electrical, Mechanical and Mechatronics Systems, Faculty of Engineering, University of Technology, Sydney, PO Box 123, Broadway, NSW 2007, Australia

Nga.Hoang@eng.uts.edu.au

**School of Electrical, Computer and Telecommunications Engineering, University of Wollongong, Northfields Avenue, NSW 2522, Australia

*** Institute of Mechanics, 264 Doican, Hanoi, Vietnam

Abstract

The effect of damping of magnetorheological elastomer (MRE) on effectiveness of Adaptive Tuned Vibration Absorber (ATVA) for vehicle powertrain torsional steady vibration reduction is presented in this study. The MRE used to develop the ATVA is a soft MRE with a significant MR effect (the increase in elastic modulus is about 100 times). Thus, the ATVA can work in a wide frequency bandwidth. Several damping models were used for the soft MRE to estimate and compare the ATVA effectiveness for vibration reduction of a powertrain which is modeled as a four-degree-of-freedom system. Also, approximated formulas for both shear modulus and damping are proposed for ATVA design and they are in agreement with experiment data. The numerical simulations of the powertrain system fitted with the ATVA are carried out for these damping models. The obtained results show that at the resonant frequency the less MRE damping ratio is the higher ATVA effectiveness could be. However, the results also indicate that a low damping ratio may result in high vibration responses at the two new invariant frequencies which are introduced after adding the ATVA to the powertrain system. Furthermore, the results showed that it is different from traditional absorbers for tuning ATVA damping ratio and stiffness coefficient because for ATVA using MREs when either stiffness or damping coefficient is tuned, the other one will be set automatically as well. This result will be useful for choosing an optimal MRE material for constructing a smart ATVA for powertrain vibration reduction.

Key words: damping, magnetorheological elastomer, adaptive tuned vibration absorber, vehicle powertrain, vibration suppression

1. Introduction

Magnetorheological elastomer (MRE) is one kind of smart material whose elastic modulus can be properly controlled by an external magnetic field. Thus, MRE has been a potential material for developing ATVAs (Adaptive Tuned Vibration Absorbers) [1, 2,3].
Hoang et al [4] used a soft MRE presented by Abramchuk et. al.[5] for developing an ATVA for vehicle powertrain vibration reduction. The results show that the ATVA can work effectively for a

wide frequency range from about 7 to 70 Hz. However, the effect of the MRE damping property to the ATVA effectiveness has not been fully addressed because the damping ratio used to validate ATVA effectiveness is only model from Zhou[1] and it was not compared to the others, which were reported.

This paper aims to use several damping property models for the soft MRE presented by Abramchuk et al. al.[5] to estimate and compare the effectiveness of ATVA based on this MRE. The numerical simulations are carried out to find out the effect of these damping models on ATVA effectiveness. This simulation will be useful for choosing an optimal MRE material for developing an ATVA for powertrain vibration control.

2. Damping models of Magnetorheological elastomers

In this section, three damping models, which were experimentally validated, will be used and they were denoted as model A, model B and model C. These models were proposed by Zhou[1], Kallio[2] and Chen et al. [3], respectively. While Model A and model B are linear functions relative to magnetic flux intensity B, model C is approximated as a cubic polynomial in this study.

2.1 Model A

Zhou[1] tested a MRE with 27% ferrous particles by volume embedded in a silicone rubber matrix and showed that the damping ratio is a slightly decreasing line (less than 10%) when the magnetic field flux intensity B increases. According to this author, the zero-field damping ratio ς_0 =0.24 was measured. Thus, this model can be expressed as follows:

$$\varsigma = \varsigma_0 - \eta B \tag{1}$$

Where η is a coefficient. This model will be determined if two conditions, for example ς_0 , $\varsigma\ (B_{\max})$ were given and the damping ratio can be expressed as

$$\varsigma = \varsigma_0 - \frac{\varsigma_0 - \varsigma\ (B_{\max})}{B_{\max}} B \tag{2}$$

2.2 Model B

By contrast to Zhou[1], Kallio[2] tested MREs and reported that the damping ratio of MRE and magnetic field flux intensity increase together if the volume fraction exceed 15%. And the damping ratio reaches the maximum value 0.26 at 27% volume fraction of ferrous particles when B=0.3T while ς_0 =0.12 to 0.16 were measured. Thus, the second model as follow can be proposed:

$$\varsigma = \varsigma_0 + \beta B \tag{3}$$

Like model A, the coefficient β can be obtained if ς_0 and $\varsigma(B_{\max})$ were known and equation (3) can be rewritten as:

$$\varsigma = \varsigma_0 + \frac{\varsigma\ (B_{\max}) - \varsigma_0}{B_{\max}} B \tag{4}$$

It is noted that the model A and model B are the same in term of mathematic formula but it is different from the physics meaning. While model A is decreasing, model B is increasing relative to magnetic flux intensity B.

2.3 Model C

It is different from damping model of MREs reported so far. Chen et al.[3] reported that MRE damping ratio and magnetic flux intensity B increases together until the damping ratio reaches a maximum value at a critical value of magnetic flux intensity B_C and then it decreases slightly. Thus, in this study, for more convenience, a cubic polynomial is approximated to describe the damping ratio as below:

$$\varsigma = a_0 + a_1 B + a_2 B^2 + a_3 B^3 \tag{5}$$

where a_i, i=0..3 is the coefficients. These coefficients can be determined from four given conditions ς_0, $\varsigma(B_{\max})$, $\varsigma(B_C) = \varsigma_{\max}$, and $\varsigma'(B_C) = 0$. From these conditions, it is straightforward to obtain vector of coefficients as below:

$$\begin{pmatrix} a_0 \\ a_1 \\ a_2 \\ a_3 \end{pmatrix} = \begin{bmatrix} 1 & 0 & 0 & 0 \\ 1 & B_{\max} & B_{\max}^2 & B_{\max}^3 \\ 1 & B_C & B_C^2 & B_C^3 \\ 0 & 1 & 2B_C & 3B_C^2 \end{bmatrix}^{-1} \begin{pmatrix} \varsigma_0 \\ \varsigma(B_{\max}) \\ \varsigma_{\max} \\ 0 \end{pmatrix} \tag{6}$$

Mathematically, the condition that the damping ratio ς is increasing $\forall B \subset [0 \; B_C]$ and decreasing $\forall B \subset [B_C \;\; B_{\max}]$ must be satisfied. In practise, $\varsigma'(0) > 0$ and $\varsigma'(B_{\max}) < 0$ are checked.

Model C is validated by experiment data. Three samples of MRE reported by Chen et. al.[3] are compared to the proposed model. These samples have the same ingredient components by weight (30% of polymer matrix, 10% of plasticizers and 60% of ferrous particles) and they are based on polymer matrix Natural rubber (NR), silicone rubber (SiR) or Chloroprene rubber (CIIR), respectively. The comparison between proposed model and experiment data are shown as in Figure 1. It can be seen the proposed model is in agreement with the experiment data.

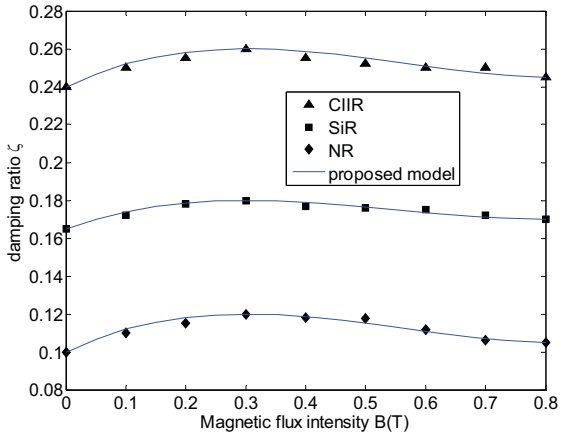

Fig. 1 Proposed model of MRE damping ratio compared to experiment data (from Chen et. al. [3])

Obviously, it is effective to obtain an instant of damping model C. For example, if a set of B_C, B_{max} and vector $\mathbf{v} = [\varsigma_0 \;\; \varsigma_{\max} \;\; \varsigma(B_{\max})]$ is given, a damping model will be obtained by equation (5). To be specific, if B_C=0.3T, B_{max}=0.8T and $\mathbf{v} = [0.1 \;\; 0.12 \;\; 0.11]$, the model will become one based on NR reported by Chen et. al.[3] and shown in Figure 1. Similarly, if $\mathbf{v} = [0.165 \;\; 0.18 \;\; 0.17]$ or $\mathbf{v} = [0.24 \;\; 0.26 \;\; 0.245]$ the model will be the damping ratio of MRE elastomer based on SiR or CIIR, respectively.

3. ATVA using a soft MRE for powertrain vibration suppression

3.1 A soft MRE material

Abramchuk et al.[5] presented a soft MRE sample that has a large MR effect (the increase in shear modulus about 100 times) in a magnetic flux intensity B_{max}=0.5T. This MRE sample based on a silicone matrix and ferrous particles with volume concentration is 27.6% and 75% plasticiser by weight fraction relative to polymer matrix. Although the shear modulus of this

material was given numerically, for more convenience, in this study a approximation is used to model the shear modulus like damping ratio model. However, it is different to damping model, the shear modulus G reaches minimum and maximum values at magnetic field flux intensity B=0 and B=B_{max}, respectively. Thus, the shear modulus of the soft MRE can be modeled as a cubic polynomial as below:

$$G = \begin{cases} G_0 & B \le 0 \\ G_0 + \sum_0^3 a_i B^i & 0 < B < B_{\max} \\ G_{\max} & B \ge B_{\max} \end{cases} \quad (7)$$

where c_i, i=0..3 is the coefficients. These coefficients can be determined from four conditions as $G(0) = G_0$, $G(B_{\max}) = G_{\max}$, $G'(0) = 0$, $G'(B_{\max}) = 0$.

With some calculation, it is straightforward to obtain:

$$G(B) = \begin{cases} G_0 & B \le 0 \\ G_0 + (G_{\max} - G_0)(\frac{B}{B_{\max}})^2 (3 - 2\frac{B}{B_{\max}}) & 0 < B < B_{\max} \\ G_{\max} & B \ge B_{\max} \end{cases} \quad (8)$$

The proposed model and experiment data of shear modulus of soft MRE are shown in Figure 2 in term of logarithm of the relative change (G/G_0) relative to the magnetic field intensity H. It can be seen that the proposed model and experiment data are in agreement. It is noted that G_0 is the initial shear modulus without magnetic field, G_0=3.5kPa and G_{max}=350kPa at B_{max}=0.5T in this case.

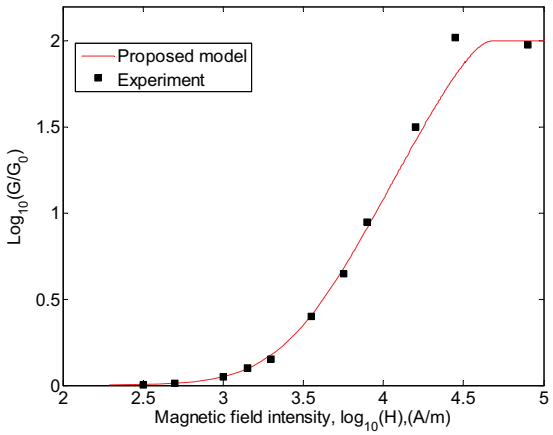

Fig. 2 Proposed model of MRE shear modulus compared to experiment data (Abramchuk et. al. [5])

It can be seen that the saturated magnetic field intensity H_S at which the shear modulus is saturated is about 50-70kA/m (B_S ~0.3-0.4T) and this point does not relate to the critical value of magnetic flux intensity B_C, which was described in damping model C.

It is noted that the damping property of this soft MRE has not been reported yet while the damping affects significantly to effectiveness of dynamic absorbers. In this paper, Model A, B and C will be used to for the soft MRE, which is used for developing an ATVA.

For the soft MRE, the maximum magnetic flux intensity B_{max}=0.5T and it is different from that of the magnetic field as shown in Figure 1 (B_{max}=0.8T). Here, model A, model B and model C are given as below:

- Model A: ς_0 =0.24, ς ($B_{\max}$)=0.216
- Model B ς_0 =0.12, ς ($B_{\max}$)=0.26
- Model C: vector $\mathbf{v} = [0.165 \;\; 0.18 \;\; 0.17]$ (based on SiR matrix) and B_C=0.2T.

These models are shown in Figure 3 and they will be used as damping ratio of the proposed

ATVA to validate its effectiveness for powertrain torsional vibration reduction.

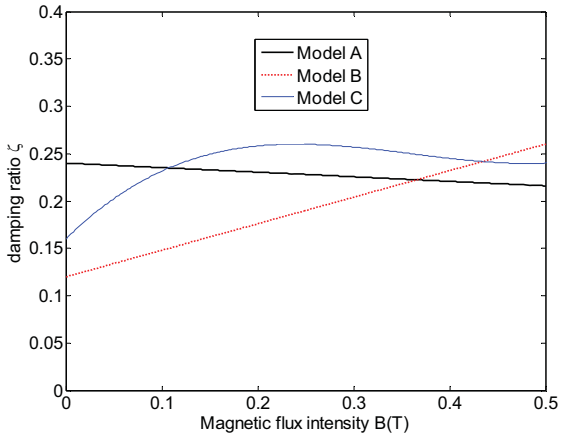

Fig. 3. Damping ratio models are used for ATVA validation

The numerical simulations of the powertrain system fitted with the ATVA are carried out for these damping models in next section.

3.2 A powertrain system

A simplified powertrain torsional vibration model is shown in Figure 4 to validate the ATVA effectiveness. This model consists of inertias, stiffnesses, and dampings. In this Figure, the vehicle engine, torque converter (TC) and the gear box and the drive line are modelled as the first inertia, second, third inertias and fourth inertia, respectively.

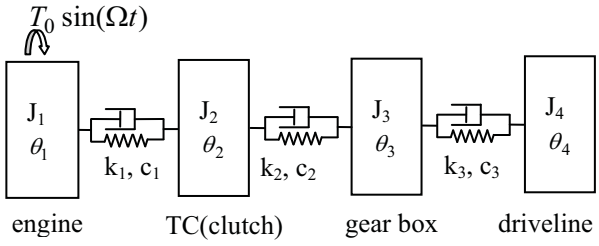

Fig.4 A simplified vehicle powertrain model (Hoang et. al.[4])

Each gear ratio of gear box has a different stiffness coefficient and this is characterized by a varying stiffness coefficient k_2.

The equation of motion of the system can be obtained easily by using Lagrange's equation as below:

$$\mathbf{J}\ddot{\boldsymbol{\theta}} + \mathbf{C}\dot{\boldsymbol{\theta}} + \mathbf{K}\boldsymbol{\theta} = \mathbf{T} \tag{9}$$

Where $\boldsymbol{\theta} = [\theta_1 \ \ \theta_2 \ \ \theta_3 \ \ \theta_4]^T$, $\mathbf{T} = [T_0 \sin(\Omega t) \ \ 0 \ \ 0 \ \ 0]^T$ are vectors of generalized coordinates and external torque. The inertial matrix J and stiffness matrix K have following forms:

$$\mathbf{J} = \begin{bmatrix} J_1 & 0 & 0 & 0 \\ 0 & J_2 & 0 & 0 \\ 0 & 0 & J_3 & 0 \\ 0 & 0 & 0 & J_4 \end{bmatrix}, \mathbf{K} = \begin{bmatrix} k_1 & -k_1 & 0 & 0 \\ -k_1 & k_1 + k_2 & -k_2 & 0 \\ 0 & -k_2 & k_2 + k_3 & -k_3 \\ 0 & 0 & -k_3 & k_3 \end{bmatrix} \tag{10}$$

The damping matrix **C** has the same form as the stiffness matrix **K.**

It was assumed that from equation (9) the vibration of powertrain could be obtained, such as natural frequencies, damped frequencies, frequency responses.

With J_1=0.82, J_2=0.22, J_3=0.4, J_4=8kgm^2; c_1=1.0, c_2=2.0, c_3=5.0Nms/rad; k_1=15000,

k_3=3350Nm/rad. And k_2=13000, 15000, 16000 and 18000 Nm/rad was set for the first, second, third and fourth gear of gear box are used, respectively. Table 1 shows the powertrain natural frequencies and damping ratios ζ for four gears of gear box.

Table 1. Natural frequencies of a simplified powertrain model for different gear shifts.

	first gear		second gear		third gear		fourth gear	
index	f (Hz)	ζ (%)	f (Hz)	ζ (%)	f (Hz)	ζ (%)	f (Hz)	ζ (%)
f_1	0[a]		0[a]		0[a]		0[a]	
f_2	7.5299[b]	2.89	7.5937	2.96	7.6199	2.99	7.6640	3.04
f_3	28.0366	3.27	28.7146[b]	3.05	29.0034	2.97	29.5017	2.82
f_4	62.3363	2.39	64.8331	2.35	66.0662	2.32	68.4972[b]	2.27

Reprinted from: Hoang et. al., (4), pp 4

Obviously, powertrain natural frequencies are various as shown in Table 1. If a powertrain natural frequency is close to or coincides with the excitation frequency, the resonance happens. In this case, the ATVA is used to deal with the resonance. It is noted that the ATVA is considered to work effectively if the powertrain resonant frequency is shifted away from the excitation frequency so that powertrain vibration is reduced significantly.

3.3 A torsional ATVA for powertrain vibration control

Hoang et. al. [4] proposed an ATVA with schematic diagram is shown in Figure 5, in which the inner cylinder with lugs is fixed on the rotating shaft. The MRE material operates as a torsional spring and it is put into the gap between the inner and outer cylinder. Like the inner cylinder, there are lugs on the outer cylinder. These lugs cause tangent elastic forces as well as elastic torque between these cylinders. Therefore, the outer cylinder can vibrate to the inner cylinder. There are three identical magnetic circuits, which are supplied by a DC current to make a magnetic field through the MRE layer. Each of the circuit consists of an electromagnetic coil and a steel core to produce high magnetic field.

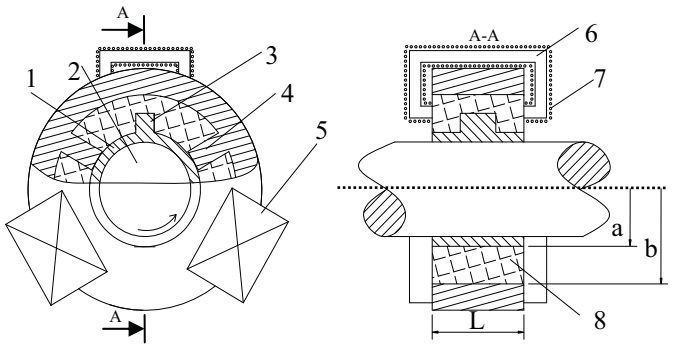

Fig.5 ATVA schematic diagram. 1: inner cylinder; 2: rotating shaft; 3, 4: lugs in inner and outer cylinders; 5: electromagnetic circuit; 6: steel core; 7: coil; 8: MRE material.

According to Hoang et. al. [4], if the MRE is modeled as a rubber cylinder with inner, outer radius and length as a, b and L, respectively as shown in Figure 5, ATVA inertia moment and stiffness coefficient can be calculated by:

$$k_A = \frac{4\pi L a^2 b^2 G}{b^2 - a^2} \tag{11}$$

$$J_A = m(b^2 + \frac{3m_{Wire}}{m} d^2) = mR_0^2 \tag{12}$$

Where m, m_{Wire} are masses of the outer ring and one wire coil, respectively; d is the distance from the mass centre of coil to the rotating shaft centre; R_0 is the equivalent radius of gyration ATVA. For instant, if m=2kg, b=0.1m, m_{Wire}/m=0.25, d=0.2m are

given, R_0=0.2m, J_A =0.08kgm^2 and $\mu_A = J_A / J_3$ =0.2 are calculated. For more convenience, the inertia ratio μ_A is varied to investigate the ATVA effectiveness. ATVA natural frequency and damped frequency are calculated by:

$$f_A = \frac{1}{2\pi}\sqrt{\frac{k_A}{J_A}} \tag{13}$$

$$f_d = f_A\sqrt{1-\varsigma_A^2} \tag{14}$$

ς_A is the damping ratio of MRE and it is chosen from either of model A, model B or model C and the ATVA damping coefficient can be calculated as below:

$$c_A = \varsigma_A C_c \tag{15}$$

$C_c = 4\pi f_A J_A$ is the critical damping coefficient.

If ATVA parameters a=0.095m, b=0.1m, L=0.04m were chosen, ATVA natural frequency f_n and its damped frequencies f_d are shown in Figure 6. Here inertia ratio μ_A =0.2 was set and the three damping models were shown in Figure 3.

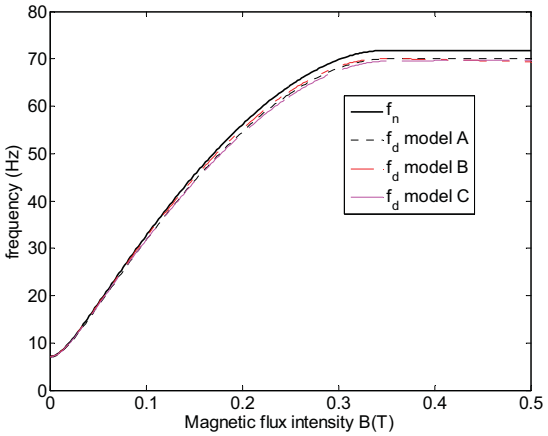

Fig.6 ATVA natural and damped frequencies

It can be seen that ATVA frequencies cover all powertrain natural frequencies as shown in Table 1. Next section will validate ATVA effectiveness for powertrain vibration control.

4. A numerical simulation

In this section, resonances happening with either f_2=7.5299Hz or f_3=28.7146Hz as noted in Table 1 will be examined. Hoang et. al.[4] reported that for resonances, which happen to these frequencies, the ATVA can work effectively if it is added to powertrain as in Figure 7.

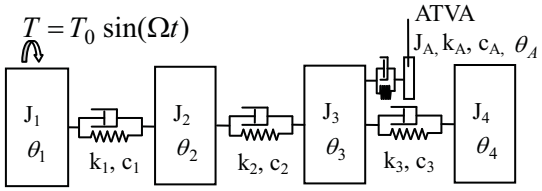

Fig.7 A powertrain model with an ATVA.

Obviously, when ATVA is added to powertrain, the equation of motion of system has the same form as equation (9) though matrices **J**, **K**, **C** are changed. Also, magnetic flux intensity B is tuned for controlling ATVA frequency f_d. When a value f_d^* is tuned, from equations (13) the magnetic flux intensity B^* will be obtained by solving a nonlinear equation (uses *fzero* function in Matlab for example). The conversion among ATVA parameters such as k_A, f_A, f_d, ς_A, c_A is through equations (11), (13), (14) and (15). Thus, matrices **J**, **K**, **C** in equation (9) will be re-calculated and then vibration of powertrain fitted with ATVA could be obtained.

4.1 Using ATVA for first gear of gear box

Hereafter, it is assumed excitation frequency of fluctuation torque Ω is a half of engine frequency. If the engine is at idle speed (about 900rpm) it gives $\Omega = 2\pi \times 7.5$ (rad/s). When the first gear of gearbox is operated, the resonance may occur to the second frequency f_2=7.5299Hz of the first gear as noted in Table 1. Thus the ATVA is used to deal with the resonance.

If ATVA frequency f_d=7.5Hz is tuned. If model B of MRE damping is chosen, from equation (5), magnetic flux intensity B=0.067T is solved, and then $\varsigma = 0.1219$ is obtained. Thus, ATVA stiffness and damping coefficient k_A and c_A are calculated. Powertrain vibration responses are shown in Figure 8 with magnitude of fluctuation torque T_0=3Nm was set.

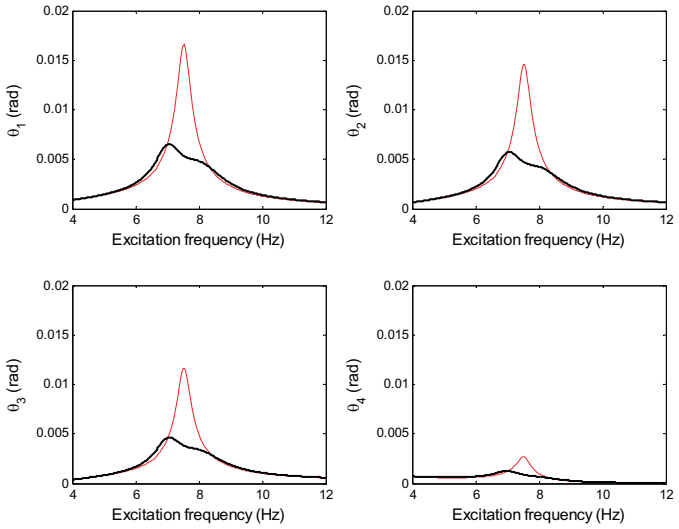

Fig.8 Powertrain vibration response before and after adding ATVA for damping model B

Obviously, after adding the ATVA, the powertrain vibration (bold lines) are reduced significantly at and around the resonant frequency f_d=7.5z compared to those of powertrain before adding ATVA (normal lines). In other words, the resonance has been shifted to be two new invariant peaks (two local maxima) so that the ATVA worked well.

To compare how the damping model A, B and C affect to ATVA effectiveness, the powertrain responses with three damping models are shown in Figure 9. For f_d=7.5Hz magnetic flux intensity B and damping ratio ς are (0.0081T, 0.2396), (0.0067T, 0.1219), (0.0071T, 0.1670) for model A, model B, model C, respectively.

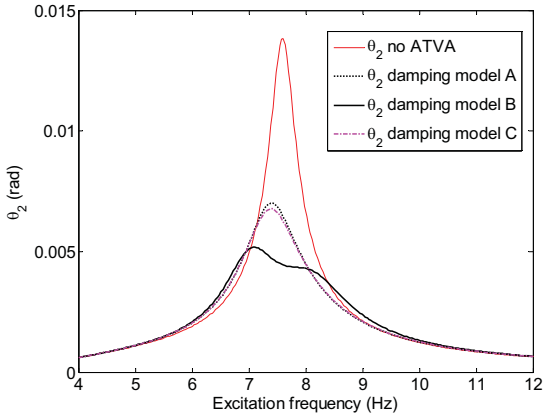

Fig.9 Vibration of second inertia θ_2 for three damping models

It can be seen that model B is the best compared to the others because around resonant frequency (f_d=7.5Hz) and at two local maxima the vibration is smallest in this case. It can be

seen that at the resonant frequency, the less MRE damping ratio is the higher ATVA effectiveness could be. However at the two local maxima, it is different. For example, if ATVA frequency f_d=7.3Hz (observed as optimal value as in Figure 11) was set and it is assumed that if by some way the damping ratio of model B can be reduced a half. That is ς_0 =0.06, ς ($B_{\max}$) =0.13. The vibration response of second inertia with different damping ratio values is shown in Figure 10.

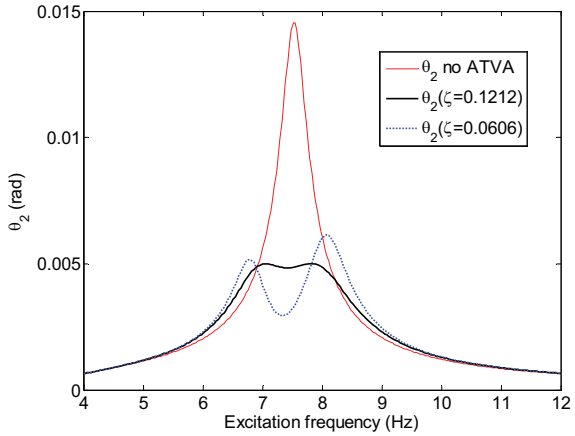

Fig.10 Responses of the second inertia for two instants of damping ratios of model B

To show how the ATVA frequency affects to its effectiveness. The frequency vibration response of the second inertia, θ_2 , is shown in Figure 11. For this case, f_d=7.2, 7.3, 7.5, 7.6 Hz were set.

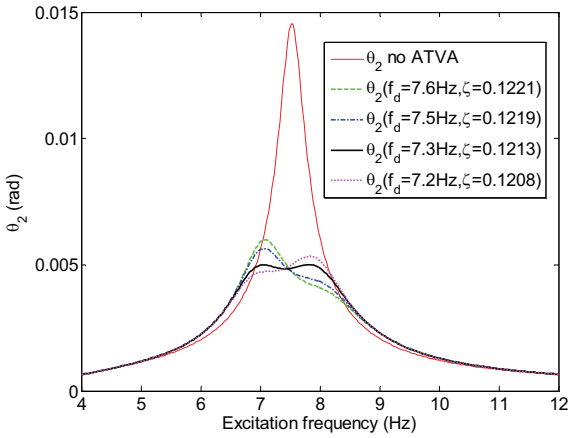

Fig.11 Vibration of second inertia θ_2 with several ATVA frequencies

It can be seen that if f_d=7.3Hz (refer to bold line in Figure 11), the ATVA effectiveness seems to be optimal because the frequency responses at the two local maxima are the same. It is noted that it is different from traditional ATVA when ATVA stiffness and damping can be tuned independently while for ATVA using MRE in this case when a MRE stiffness coefficient is tuned its damping coefficient will be set automatically.

4.2 Using ATVA for second gear of gear box

In this case the engine speed is assumed to operate at 3420 rpm that means the excitation frequency of fluctuation torque is 28.5Hz such that the resonance happens with f_3=28.7146 Hz. If f_d=28Hz is tuned, models A, B and C will be calculated as below:

- Model A: magnetic field flux intensity B=0.0863T, ς =0.2359
- Model B: B=0.0845T, ς =0.1437
- Model C: B=0.0861T, ς =0.2247.

The frequency response of third inertia, θ_3, is shown in Figure 12 for three damping

models A, B, and C with T_0=30Nm was set.

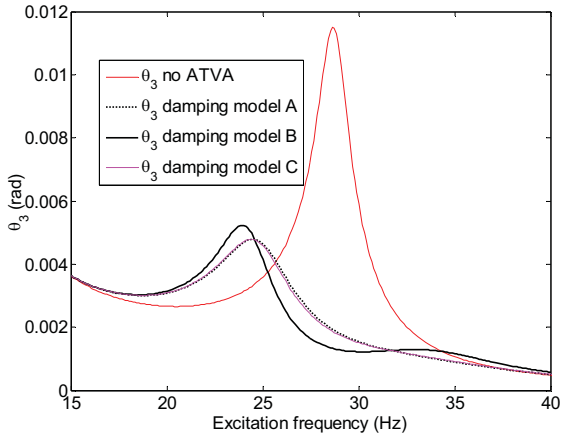

Fig.12 Vibration of third inertia θ_3 with three damping model and damping models

Obviously, after adding ATVA to the powertrain, the resonant frequency f=28Hz is shifted away so that the vibration response at and around this resonant frequency is reduced significantly either damping model is Model A, Model B or model C. In this case the difference among vibration level for these damping models is slight.

6. Conclusion

In this paper, three MRE damping models were used for a soft MRE, whose MR effect is significant, to investigate the ATVA effectiveness. Formulas are approximated for modeling of damping ratio as well as shear modulus (or stiffness). The approximations are experimentally validated with experiment data and they are effective for ATVA design. The obtained results show that at the resonant frequency the less MRE damping ratio is the higher ATVA effectiveness could be. However, a low damping ratio may results in high vibration responses at the two new invariant frequencies which are introduced after adding the ATVA to the powertrain system. Furthermore, it is different from traditional dynamic absorbers for the ATVA that its stiffness and damping coefficients are tuned together. The parameter optimization of ATVA using MRE will be discussed in further work.

7. References

(1) Zhou G Y, Shear properties of a magnetorheological elastomer, Smart Material and Structure, 12, 2003, pp. 139-46

(2) Kallio M, The elastic and damping properties of magnetorheological elastomers, 2005, VTT publications, Finland.

(3) Chen L, Gong X, Li X, Damping of Magnetorheological Elastomers Chinese Journal Chemistry Physics, 21, 2008, pp.581-585

(4) Hoang N, Zhang N and Du H, A dynamic absorber with a soft magnetorheological elastomer for powertrain vibration suppression, Smart Material and Structure, 18(7), 2009.

(5) Abramchuk S S, Grishin D A, Kramarenko E Y, Stepanov G V and Khokhlov A R 2006 Effect of a homogeneous magnetic field on the mechanical behavior of soft magnetic elastomers under compression, Journal of Polymer Science, Part A, 48(2), 2006, pp.138-145